Self-Powered n-SnO$_2$/p-CuZnS Core–Shell Microwire UV Photodetector with Optimized Performance

Jian Cai, Xiaojie Xu, Longxing Su, Wei Yang, Hongyu Chen, Yong Zhang, and Xiaosheng Fang*

Herein, a single-crystal SnO$_2$ microwire photodetector (PD) is demonstrated with a fast response speed owing to a low concentration of point defects. However, the presence of surface defects (e.g., oxygen vacancies) still limits its optoelectronic performance. To further improve the photoresponse of such device, a core–shell p–n junction is constructed by simply coating a new p-type transparent conductive (CuS)$_{0.35}$:(ZnS)$_{0.65}$ nanocomposite film (CuZnS) on n-type SnO$_2$ microwire. As a result, not only the surface of SnO$_2$ is modified, but also a space charge depletion region is formed at the interface, leading to an enhanced on-off ratio of $\approx 1.3 \times 10^3$ and a faster speed of 45 µs/1.17 ms (rise time/decay time) in comparison with the plain SnO$_2$ microwire PD (on-off ratio of 30, response speed of $\approx$100 µs/1.5 ms). Besides, the n-SnO$_2$/p-CuZnS core–shell microwire could steadily work as a self-powered UV PD, with a maximum responsivity of 1.6 mA W^{-1} (at 0 V) and detectivity of 5.41×10^{11} Jones (at 0.05 V) toward 315 nm, which suggests its great potentials as a high-performance self-powered UV photodetector.

As eyes are to human beings, so are sensors to information technology. Ultraviolet photodetectors (UV PDs), which could easily detect UV irradiations by converting optical information into electrical signals based on photoelectric effect, have been extensively used in applications such as environmental monitoring, biological/chemical analysis, flame detection, ultraviolet communications, etc.[1–6] In general, there are two common approaches to realize UV detection: photoconductive effect and photovoltaic effect. Frankly speaking, the photoconductive PDs work via the majority carriers circulating through an external circuit for many times, thus typically achieving a high photogain. However, it usually suffers from a slow recovery speed due to the persistent photoconductivity (PPC) effect, which means its conductivity keeps increasing when the light is off due to the presence of intrinsic defects.[7–9] Moreover, some conventional material candidates for UV photodetection, such as metal oxides: ZnO and TiO$_2$, even show a longer recovery time due

to the long chemical readsorption process (oxygen molecules readsorption) occurred at the surface.[10,11] In contrast, the photovoltaic PDs including p–n homojunctions, p–n heterojunctions, and Schottky barrier diodes show a fast response speed and a possible self-powered function due to the photovoltaic effect. Furthermore, as there is an increasing emphasis on low energy consumption, self-powered PDs which can operate without an external power source are particularly appealing in applications like submarine oil leakage monitoring and forest fires prevention.[12] Thus, researchers are highly motivated to develop high-performance UV PDs with self-powered characteristics.

Thanks to the continuous innovations in semiconductor technology, various wide-bandgap materials such as diamond, ZnO, TiO$_2$, ZnS, etc., have drawn great attention in the field of UV PDs.[13–16] Among them, SnO$_2$, a conventional metal oxide with a direct bandgap, is generally regarded as a n-type material in its undoped form because of the intrinsic defects. It possesses unique chemical, electrical, and optoelectronic properties, thus having vast applications in gas sensors, transparent conductors, and optoelectronic devices.[17–19] In particular, with a wide bandgap of $\approx$3.6 eV (at 300 K), SnO$_2$ exhibits good UV light absorption characteristics and high visible light transparency, making it an ideal candidate for UV PD, especially under acidic or alkalic circumstances in comparison with ZnO.[20] Up to now, various efforts have been devoted to demonstrate the excellent UV photosensitivity of SnO$_2$. Previously, our group presented thin SnO$_2$ nanowire UV PDs with a high external quantum efficiency.[21] Chen et al.[22] fabricated monolayer SnO$_2$ nanonets with a high UV photocurrent. Tian et al.[23] reported ZnO-SnO$_2$ heterojunction nanofibers with a high UV photo-dark current ratio. However, the response time of the works mentioned above is still dissatisfactory, of which the decay time is >50 s,[22] $\approx$50 s,[21] and 7.8 s,[23] respectively. Recently, Ling et al.[24] constructed a SnO$_2$ nanoparticle thin film/SiO$_2$/p-Si heterojunction, which exhibited a short response time (<0.1 s) and a high UV photocurrent ($\approx$4.0 × 10^{-5} A), however, it suffered from a low photosensitivity ($\approx$40) due to the high dark current. Thus, a combination of a high photosensitivity and a fast response speed has not been realized in SnO$_2$ PDs, not to mention additional functions including self-powered property and flexibility.

J. Cai, Dr. X. J. Xu, Dr. L. X. Su, W. Yang, Dr. H. Y. Chen,
Dr. Y. Zhang, Prof. X. S. Fang
Department of Materials Science
Fudan University
Shanghai 200433, P. R. China
E-mail: xshfang@fudan.edu.cn

ADVANCED
SCIENCE NEWS
www.advancedsciencenews.com

ADVANCED
OPTICAL
MATERIALS
www.advopticalmat.de

Herein, we synthesized single-crystal SnO$_2$ microwires via a typical vapor transport process. They exhibit a photoresponse speed of 100 μs/1.5 ms (rise time and decay time) at a bias of ≈3 V, which is much faster than the previous reports on SnO$_2$ PDs. The superior response speed may be attributed to its high crystallinity that favors for a higher charge mobility and transport process. However, PPC effect still exists as it takes quite a long time for the device to revert to its original dark current. A facile chemical-bath-coating of a p-type transparent conductive CuZnS nanocomposite film would not only help modify the surface of SnO$_2$ microwires, but also form a p–n heterojunction, thus leading to an improved response speed of SnO$_2$ PD and may endow it with a self-powered property. The as-prepared SnO$_2$/CuZnS core–shell microwire shows a higher photosensitivity (on-off ratio of ≈1.3 × 10^3 at 3 V) and a faster response speed (rise time of 45 μs and decay time of 1.17 ms) in contrast to SnO$_2$ microwire PD. Moreover, it could operate without an external power source, namely, it could steadily work as a self-powered UV PD, along with a maximum responsivity of 1.6 mA W^{-1} (0 V) and detectivity of 5.41 × 10^{11} Jones (0.05 V) at 315 nm. All of these characteristics indicate that the optoelectronic properties of our device are superior to other SnO$_2$-based PDs in literature, and even comparable to the state-of-the-art self-powered PDs.[25–28]

Figure 1a,b shows the scanning electron microscopy (SEM) images of SnO$_2$ microwires prepared via a typical vapor transport process. The surface is smooth, suggesting that high-quality SnO$_2$ microwires are obtained. Those microwires are uniform along the longitudinal direction with a length of up to 1 cm. They have rectangular cross sections with an average size of ≈10 μm. The X-ray diffraction (XRD) pattern from a single SnO$_2$ microwire is shown in Figure 1c. It exhibits a strong and sharp diffraction peak at 34.3°, corresponding to the (101) crystal face of rutile SnO$_2$, suggesting the as-obtained SnO$_2$ microwire possesses a single-crystal structure. This is also confirmed by the selected-area electron diffraction (SAED) pattern (Figure S1, Supporting Information), which also indicates that microwires grew along the crystal direction of [010].

In order to investigate the optoelectronic characteristics of the as-grown SnO$_2$ microwires, a SnO$_2$ microwire UV PD (diameter of ≈12 μm) was fabricated by manually patterning indium (In) contacts at both ends, as schematically illustrated in **Figure 2**a. The linear I–V curve in Figure S2a (Supporting Information) indicates that In formed an ohmic contact with SnO$_2$, suggesting the constructed device is a photoconductive UV PD. Figure 2b shows the current–voltage (I–V) characteristics of the device, the dark current of the SnO$_2$ microwire is low (≈1 pA at 1 V), which may be attributed to a relatively low concentration of point defects in single-crystal SnO$_2$ microwires. On the other hand, chemical adsorption on the surface, especially oxygen molecules adsorption by trapping free electrons [$O_2 + e^- \rightarrow O_2^-$], has formed a "space charge region" with surface defects, leading to a surface barrier that lowers the dark current.[21,29,30] This device has a negligible response toward visible light but a very strong photoresponse upon ultraviolet irradiation, for instance, the photocurrent under 300 nm illumination (1.103 mW cm^{-2}) is two orders of magnitude higher than that in dark, confirming that SnO$_2$ microwire PD is a good solar-blind UV-sensitive PD.
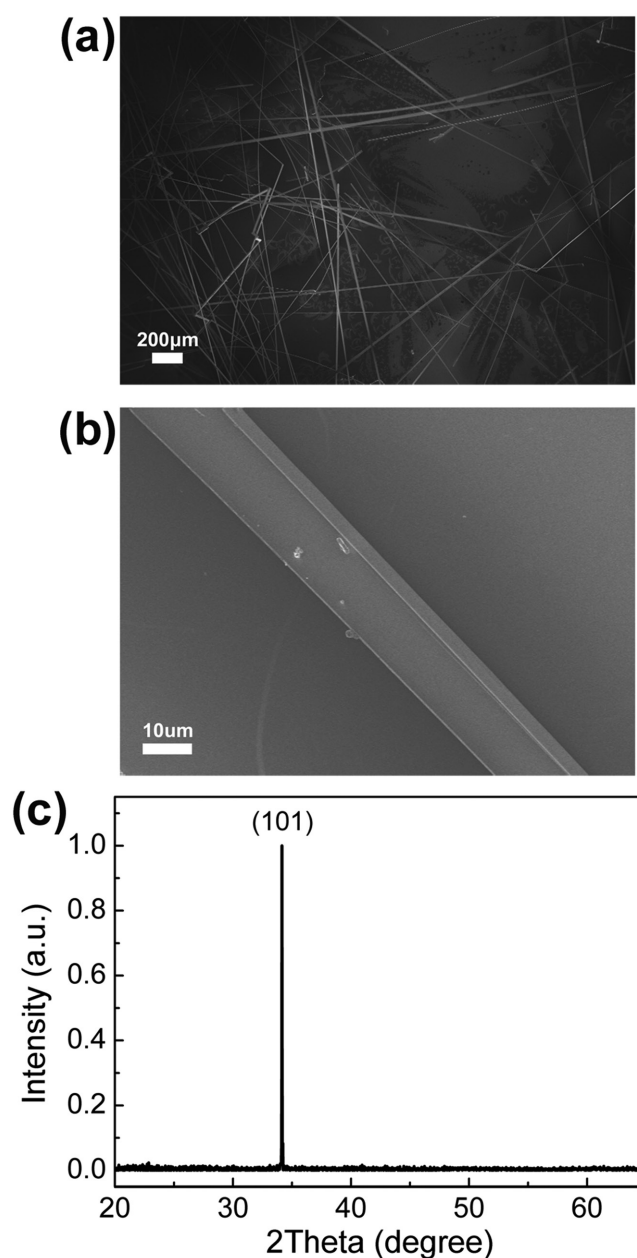

Figure 1. a,b) SEM images of as-prepared SnO$_2$ microwires. c) XRD pattern of a single SnO$_2$ microwire.

Moreover, the current–time (I–t) curve under a bias of 3 V is also presented in Figure 2c. With repeatedly turning on and off (300 nm), the current changes sensibly and remains stable under continuous illumination. However, it takes a long time to revert to its original value due to the PPC effect (Figure S3, Supporting Information), probably arising from the surface oxygen readsorption. Generally speaking, upon UV illumination, the photogenerated electron–hole (e–h) pairs are separated by surface space charges, and then the holes will emigrate to the surface which gives rise to the desorption of oxygen molecules [$O_2^- + h^+ \rightarrow O_2$], thus resulting in a notable increase of conductivity; Once the light is off, there are no continuous photogenerated e–h pairs in SnO$_2$ microwire and the electrons will be quickly trapped by
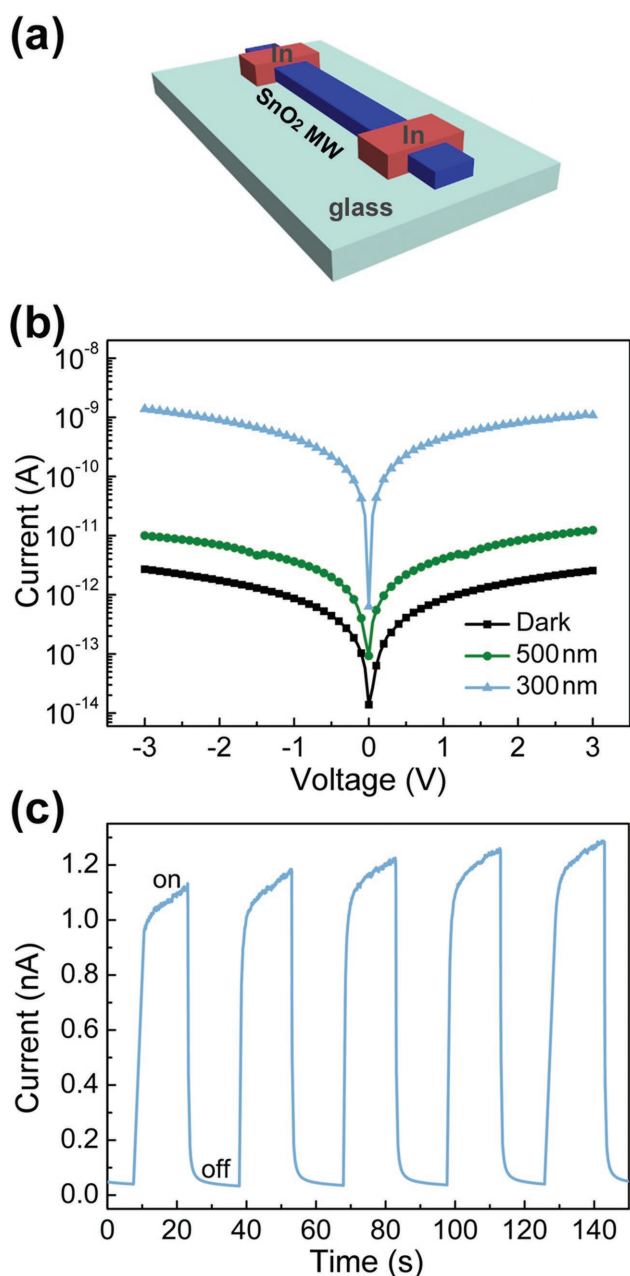
1800213 (2 of 7)

**ADVANCED
SCIENCE NEWS**
www.advancedsciencenews.com

**ADVANCED
OPTICAL
MATERIALS**
www.advopticalmat.de

(a)

(b)

(c)

Figure 2. Photoelectric performance of a single SnO_2 microwire photodetector. a) The schematic diagram of the SnO_2 microwire photodetector. b) Its I–V characteristics in a log coordinate under dark and illumination with 500 nm visible light (2.524 mW cm^{-2}), and 300 nm UV light (1.103 mW cm^{-2}). c) Its I–t characteristics with repeatedly on/off switching under 300 nm UV light illumination at a bias of 3 V.

the defects, but the long oxygen readsorption process makes it hard to revert to the original dark current. Disregarding that, it can be seen that both the decay time and rise time are less than 1 s, which are much faster than that of the previously reported SnO_2-based PDs.[21–23,31] However, it is inaccurate on account of the restriction of our current test equipment. Further test results using an oscilloscope with a pulsed YAG:Nd laser are presented later, showing a rise time of 100 µs and a decay time of 1.5 ms under an applied voltage of 3 V in Figure 4b.

Although single-crystal SnO_2 microwire UV PD exhibits merits of a low dark current and a fast response speed, it is hard to revert to the original dark current when UV light is turned off, which commonly exists in many metal oxide UV PDs due to a long process of surface readsorption of oxygen molecules.[32] On account of this, an idea of constructing p–n heterojunction comes up, where the surface modification by a p-type transparent conductor would help minimize the effect of oxygen molecules adsorption. A faster response speed and even a higher photocurrent can also be envisioned, as the built-in electric field near the p–n interference could effectively facilitate the separation of photogenerated e–h pairs.[33–35] Besides, the built-in electric field will endow it with a self-powered feature.[12]

To guarantee enough UV light absorption by the SnO_2 microwire, the p-type layer should be as "transparent" as possible. So a p-type transparent conductive CuZnS nanocomposite film, which can be easily prepared via chemical bath deposition and other methods according to our previous report,[36–39] is a good candidate. Accordingly, a SnO_2/CuZnS core–shell microwire was prepared, as shown in **Figure 3**a, the CuZnS is quite thin, enabling enough UV light absorption of SnO_2 core. The core–shell microwire was transferred to a glass substrate, followed by manually positioning In contacts on SnO_2 and CuZnS as illustrated in Figure 3b. Finally, the device was kept on the hot plate at 300 °C for 5 s to form good contacts. As both CuZnS and SnO_2 will form good ohmic contact with In electrodes, the rectifying property comes from the p–n junction of n-SnO_2/p-CuZnS (Figure S2, Supporting Information). Figure 3c presents the I–V characteristics of the device, where the photocurrent under 300 nm light illumination is much higher than that of pure SnO_2 UV PD. Interestingly, the I–t curve (Figure 3d) under a bias of 3 V exhibits a significantly enhanced on-off ratio, from 30 to ≈1.3 × 10^3, which might be resulted from the increased photocurrent and decreased dynamic dark current, suggesting that p-type CuZnS plays an important role in the photosensitivity of the device. It might be ascribed to the following reasons: (1) The charge depletion from the carriers diffusion at the p–n interface gives rise to a higher barrier at the surface, thus lowering the dark current; (2) The charge depletion region could not only effectively help separate the photogenerated charge carriers, but also suppress the recombination rate, boosting the carrier density and photocurrent; (3) The core–shell configuration makes the external voltage mainly distribute near the junction and enhances the electric field in depletion region, thus further improving the photocurrent.

Clearly, this core–shell microwire PD shows an obvious photoresponse at zero bias, indicating that the device could work as a self-powered UV PD. The I–t curve at zero bias with a periodic 300 nm light radiation is shown in **Figure 4**a. As the light is turned on or off, the current abruptly ascends to ≈18 pA or descends to its original value of 0.1 pA, leading to an on-off ratio of 180. Furthermore, the photocurrent keeps stable under continuous illumination, demonstrating that the heterojunction device could work efficiently and steadily without an external power source.

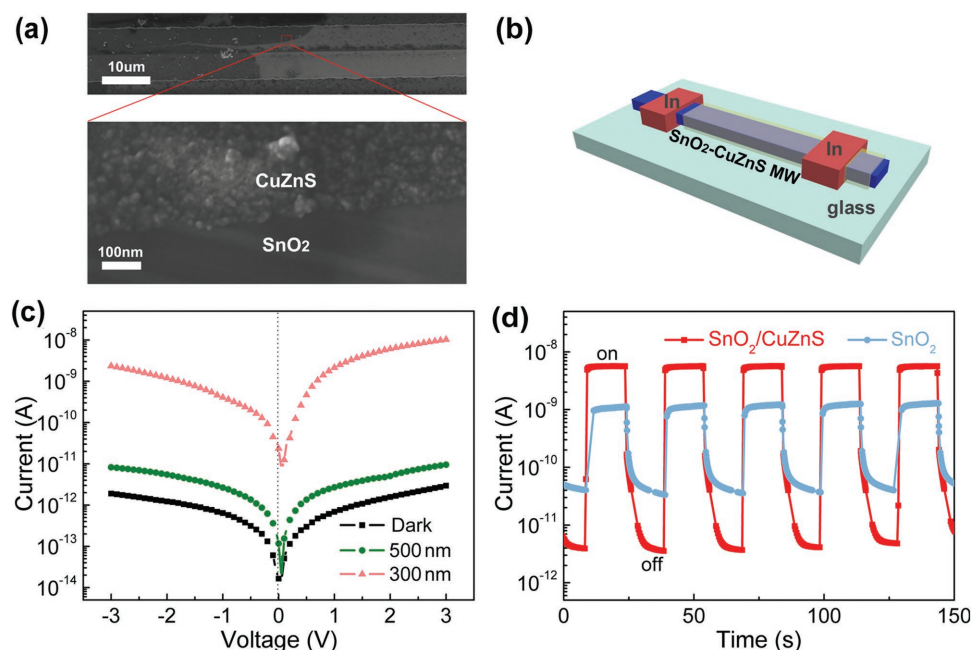Response time is a crucial parameter in UV detection. As UV PDs are widely used optoelectronic sensors, a short

Figure 3. Photoelectric performance of a single n-SnO_2/p-CuZnS core–shell microwire photodetector. a) SEM images of a single n-SnO_2/p-CuZnS core–shell microwire, the image below shows the magnification of the boundary line between the two materials. b) The schematic diagram of the device. c) Its I–V characteristics in a log coordinate under dark and illumination with 500 nm visible light (2.524 mW cm^{-2}), and 300 nm UV light (1.103 mW cm^{-2}). d) Its I–t characteristics with on/off switching under 300 nm UV light illumination at bias of 3 V in comparison to a pure SnO_2 microwire PD.
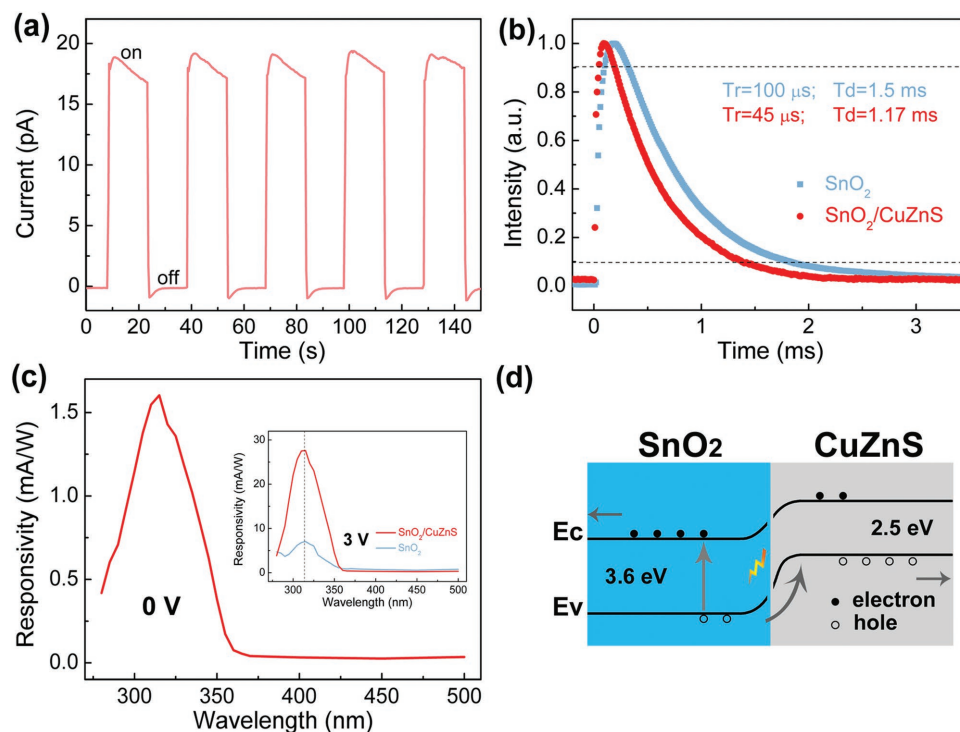

Figure 4. a) The I–t characteristics of a single n-SnO_2/p-CuZnS microwire PD with on/off switching under 300 nm UV light illumination at bias of 0 V. b) The comparision of time-resolved response under 355 nm pulse laser radiation at a bias of 3 V. c) The photoresponse spectrum of a single n-SnO_2/p-CuZnS microwire PD at the bias of 0 V, the inset shows the comparison of the responsivity under a bias of 3 V. d) The schematic energy band diagram of the heterojunction device.

**ADVANCED
SCIENCE NEWS**
www.advancedsciencenews.com

**ADVANCED
OPTICAL
MATERIALS**
www.advopticalmat.de

Table 1. The characteristic parameters of SnO_2-based UV PDs in the literature.

Photodetector	Wavelength [nm]	Bias [V]	Dark current [A]	On-off ratio	Responsivity [mA W^{-1}]	Response time [s]	Ref.
SnO_2 nanonets	320	1	9.0×10^{-5}	4	–	>50/50	[22]
SnO_2 nanowire	320	1	1.9×10^{-8}	108	–	≈50/50	[21]
ZnO/SnO_2 nanofibers	300	10	1.7×10^{-12}	4600	–	32.2/7.8	[23]
Ni-SnO_2 nanobelts	254	1	7.0×10^{-10}	1000	–	0.5/5.0	[31]
SnO_2 microrod	260	2	2.6×10^{-6}	2	–	<1/1	[8]
Zn_2SO_4/SnO_2 film	310	5	1.1×10^{-11}	1000	508	9.02/0.82	[41]
SnO_2 film/SiO_2/p-Si	365	1	≈1.0×10^{-6}	40	425	<0.1/0.1	[24]
SnO_2 microwire	300	3	4.2×10^{-11}	30	7.1 (315 nm)	0.1/1.5 ms	This work
$SnO_2/CuZnS$ microwire	300	3	4.0×10^{-12}	1300	27.6 (315 nm)	0.045/1.17 ms	This work
		0	1.0×10^{-13}	180	1.6 (315 nm)	<0.045/1.17 ms	

response time is desperately in demand for signal's acquisition. In this work, the response time of our device was accurately recorded by an oscilloscope under the excitation of pulsed YAG:Nd laser.[40] As shown in Figure 4b, the rise time (τ_r) from 10 to 90% and the decay time (τ_d) from 90 to 10% are counted to be 45 μs and 1.17 ms at a bias of 3 V, respectively. Both are shorter in comparison with that of pure SnO_2 microwire, indicating that the construction of $SnO_2/CuZnS$ p–n junction effectively promotes the response speed. It is also speculated that the response speed without an external power could be faster, in view of no carrier injection. Compared with recent reports on SnO_2-based UV PDs, the response time of our device is outstanding (**Table 1**), of which the decay time is about five orders of magnitude shorter than that of the previous report,[22] thus hopefully realizing the detection of the variations in UV light intensity at a high frequency.

As another key parameter to evaluate a PD's performance, the spectrum responsivity (R_λ) can be calculated according to the following equation

$$R_\lambda = \frac{I_{ph}}{P_\lambda} = \frac{I_\lambda - I_d}{E_\lambda S} \tag{1}$$

where I_{ph} is the photocurrent, I_λ is illumination current, I_d is the dark current, P_λ is light power, E_λ is the light power intensity, and S is the effective illuminated area. Figure 4c shows the wavelength-dependent responsivity of the core–shell microwire device at zero bias, which again confirms its superior sensitivity in UV region. The climax appears at the wavelength of 315 nm with a value of 1.6 mA W^{-1}, which is comparable to the state-of-the-art self-powered UV PDs, especially in SnO_2-based devices. Compared with the pure SnO_2 microwire PD, the core–shell microwire shows a higher responsivity in UV region and a lower responsivity in visible region under a bias of 3 V (inset of Figure 4c), presenting an improved UV spectrum sensitivity.

Hence, the core–shell device configuration plays a crucial role in enhancing the optoelectronic performance. As shown in Figure 4d, SnO_2 and $CuZnS$ form a typical type-II heterojunction at the interface. Under UV irradiation, e–h pairs are generated in the active layer of SnO_2, and then are quickly separated by the built-in electric field, where photoinduced electrons tend to migrate to the conduction band of SnO_2 while the holes will move to the valance band of $CuZnS$. Eventually, the electrons and holes will be collected by the In electrodes and form a loop current, thus it can work as an effective self-powered PD.[27,28]

Apart from maximizing the response to light, one PD's performance can also be improved by minimizing the noise effect.[7] The detectivity ($D*$) describes the smallest detectable signals of the PDs from the noise environment. On account of the major contribution to the dark current from noise, it is defined as[26]

$$D* = \frac{R_\lambda}{(2qI_d/S)^{1/2}} \tag{2}$$

In this work, $D*$ of single core–shell microwire is as high as 5.41×10^{11} Jones (0.05 V) at the wavelength of 315 nm because of high UV sensitivity and low dark current, which is comparable to other high-performance self-powered UV PDs.[25–27]

In summary, the as-synthesized single-crystal SnO_2 microwires via a typical vapor transport process show a low dark current, good UV sensitivity, and fast response speed (rise/decay time: 100 μs/1.5 ms under 3 V), but the PPC effect still exists which is probably due to surface chemisorptions, resulting in a low on-off ratio of 30. By constructing a p–n junction with a p-type transparent conductive $(ZnS)_{0.35}$:$(CuS)_{0.65}$ nanocomposite film via a facile chemical bath deposition method, not only the surface of SnO_2 is modified, but also shows a self-powered property. The as-prepared $SnO_2/CuZnS$ core–shell microwire shows enhanced optoelectronic characteristics, with an on-off ratio of ≈1.3×10^3, a rise time of 45 μs, and a decay time of 1.17 ms under a bias of 3 V. Meanwhile, it could steadily work as a self-powered UV PD, along with a maximum responsivity of 1.6 mA W^{-1} under zero bias and detectivity of 5.41×10^{11} Jones (0.05 V) at 315 nm. All of these outstanding characteristics make it a great choice for high-performance UV PDs.

Experimental Section

SnO$_2$ Microwires Synthesis: SnO$_2$ microwires were prepared via a typical vapor transport process in a horizontal tube furnace. A mixture of SnO$_2$ (99.99%) and graphite powders (99.5%) with a weight ratio of 1:1 was loaded in a ceramic boat, where an equal amount of pure SnO$_2$ powder was loaded at the downstream end, and then the ceramic was put into a small quartz tube (20 × 200 mm), which was previously cleaned and also served as substrate. The temperature was increased to 1300 °C at a rate of 25 °C min^{-1}, maintained for 1.5 h, and then declined naturally. A constant flow of Ar (99.99%) with 300 standard cubic centimeters per minute (sccm) was used as the protecting and carrier gas through the entire process. Large quantities of SnO$_2$ microwires were synthesized at the downwind end of the small quartz tube.

SnO$_2$/CuZnS Core–Shell Microwires Synthesis: Thin CuZnS film was easily prepared via solution growth as previous work.[38,39] First, the selected SnO$_2$ microwires were partially sandwiched between two clipped thermal release tapes, which lose its adhesiveness when heated >160 °C (produced by Nitto Denko Corporation). Afterward, the half-coated microwires were immersed into the solution, kept stirring properly at 80 °C for 1 h to coat a compact CuZnS film. Then, the microwires were taken out, repeatedly rinsed with alcohol and deionized water, and naturally dried for about 1 h. After that, the tapes were heated at 160 °C for 1 min to release as-synthesized SnO$_2$/CuZnS core–shell microwires, with the core partially exposed for preparation of In electrode.

Characterizations: The morphologies of pure SnO$_2$ microwires and SnO$_2$/CuZnS microwires were traced by field emission SEM (FESEM) (Zeiss Sigma). The phase was identified by XRD (Bruker D8-A25) with CuK radiation ($\lambda = 0.15406$ nm). The light intensity was measured with a NOVA II power meter (OPHIR photonics). The photoelectric properties of the PDs were recorded with the semiconductor characterization system (Keithley 4200-SCS), connected to a 75 W xenon arc lamp with a monochromator. Time-resolved responses of the devices were measured with a 1 GΩ series resistor by an oscilloscope (Tektronix MSO/DPO5000) as a previous report,[40] in which a YAG:Nd laser with pulse width of 3–5 ns (Continuum Electro-Optics, MINILITE II, 355 nm) was used as excitation light source. All the electrical tests were carried out at room temperature under ambient conditions with a controlled relative humidity of 30–40%, since SnO$_2$ is very sensitive to humidity.

Supporting Information

Supporting Information is available from the Wiley Online Library or from the author.

Acknowledgements

Conflict of Interest

The authors declare no conflict of interest.

[1] H. Y. Chen, K. W. Liu, L. F. Hu, A. A. Al-Ghamdi, X. S. Fang, *Mater. Today* **2015**, *18*, 493.
[2] X. Liu, L. L. Gu, Q. P. Zhang, J. Y. Wu, Y. Z. Long, Z. Y. Fan, *Nat. Commun.* **2014**, *5*, 4007.
[3] W. Tian, D. Liu, F. R. Cao, L. Li, *Adv. Opt. Mater.* **2017**, *5*, 1600468.
[4] Y. Ning, Z. M. Zhang, F. Teng, X. S. Fang, *Small* **2018**, *14*, 1703754.
[5] E. V. Gorokhov, A. N. Magunov, V. S. Feshchenko, A. A. Altukhov, *Instrum. Exp. Tech.* **2008**, *51*, 280.
[6] Z. Y. Xu, B. M. Sadler, *IEEE Commun. Mag.* **2008**, *46*, 67.
[7] G. Konstantatos, E. H. Sargent, *Nat. Nanotechnol.* **2010**, *5*, 391.
[8] K. W. Liu, M. Sakurai, M. Aono, D. Z. Shen, *Adv. Funct. Mater.* **2015**, *25*, 3157.
[9] E. Monroy, F. Calle, E. Munoz, B. Omnes, P. Beaumont, P. Gibart, *J. Electron. Mater.* **1999**, *28*, 240.
[10] H. Kind, H. K. Yan, B. Messer, M. Law, P. D. Yang, *Adv. Mater.* **2002**, *14*, 158.
[11] X. Z. Kong, C. X. Liu, W. Dong, X. D. Zhang, C. Tao, L. Shen, J. R. Zhou, Y. F. Fei, S. P. Ruan, *Appl. Phys. Lett.* **2009**, *94*, 123502.
[12] L. X. Su, W. Yang, J. Cai, H. Y. Chen, X. S. Fang, *Small* **2017**, *13*, 1701687.
[13] E. Monroy, F. Omnes, F. Calle, *Semicond. Sci. Technol.* **2003**, *18*, R33.
[14] H. Y. Chen, K. W. Liu, X. Chen, Z. Z. Zhang, M. M. Fan, M. M. Jiang, X. H. Xie, H. F. Zhao, D. Z. Shen, *J. Mater. Chem. C* **2014**, *2*, 9689.
[15] G. H. Liu, N. Hoivik, X. M. Wang, S. S. Lu, K. Y. Wang, H. Jakobsen, *Electrochim. Acta* **2013**, *93*, 80.
[16] X. S. Fang, Y. Bando, M. Y. Liao, U. K. Gautam, C. Y. Zhi, B. Dierre, B. D. Liu, T. Y. Zhai, T. Sekiguchi, Y. Koide, D. Golberg, *Adv. Mater.* **2009**, *21*, 2034.
[17] A. Kolmakov, D. O. Klenov, Y. Lilach, S. Stemmer, M. Moskovits, *Nano Lett.* **2005**, *5*, 667.
[18] C. Kilic, A. Zunger, *Phys. Rev. Lett.* **2002**, *88*, 095501.
[19] S. Das, V. Jayaraman, *Prog. Mater. Sci.* **2014**, *66*, 112.
[20] Z. Q. Liu, D. H. Zhang, S. Han, C. Li, T. Tang, W. Jin, X. L. Liu, B. Lei, C. W. Zhou, *Adv. Mater.* **2003**, *15*, 1754.
[21] L. F. Hu, J. Yan, M. Y. Liao, L. M. Wu, X. S. Fang, *Small* **2011**, *7*, 1012.
[22] H. Chen, L. F. Hu, X. S. Fang, L. M. Wu, *Adv. Funct. Mater.* **2012**, *22*, 1229.
[23] W. Tian, T. Y. Zhai, C. Zhang, S. L. Li, X. Wang, F. Liu, D. Q. Liu, X. K. Cai, K. Tsukagoshi, D. Golberg, Y. Bando, *Adv. Mater.* **2013**, *25*, 4625.
[24] C. C. Ling, T. C. Guo, W. B. Lu, Y. Xiong, L. Zhu, Q. Z. Xue, *Nanoscale* **2017**, *9*, 8848.
[25] L. X. Zheng, F. Teng, Z. M. Zhang, B. Zhao, X. S. Fang, *J. Mater. Chem. C* **2016**, *4*, 10032.
[26] H. Y. Chen, P. P. Yu, Z. M. Zhang, F. Teng, L. X. Zheng, K. Hu, X. S. Fang, *Small* **2016**, *12*, 5809.
[27] B. D. Boruah, A. Misra, *ACS Appl. Mater. Interfaces* **2016**, *8*, 18182.
[28] B. Zhao, F. Wang, H. Y. Chen, L. X. Zheng, L. X. Su, D. X. Zhao, X. S. Fang, *Adv. Funct. Mater.* **2017**, *27*, 1700264.

[29] C. H. Lin, R. S. Chen, T. T. Chen, H. Y. Chen, Y. F. Chen, K. H. Chen, L. C. Chen, *Appl. Phys. Lett.* **2008**, *93*, 112115.

[30] D. S. Zheng, J. L. Wang, W. D. Hu, L. Liao, H. H. Fang, N. Guo, P. Wang, F. Gong, X. D. Wang, Z. Y. Fan, X. Wu, X. J. Meng, X. S. Chen, W. Lu, *Nano Lett.* **2016**, *16*, 2548.

[31] S. Y. Huang, K. Matsubara, J. Cheng, H. P. Li, W. Pan, *Appl. Phys. Lett.* **2013**, *103*, 141108.

[32] X. S. Fang, L. F. Hu, K. F. Huo, B. Gao, L. J. Zhao, M. Y. Liao, P. K. Chu, Y. Bando, D. Golberg, *Adv. Funct. Mater.* **2011**, *21*, 3907.

[33] L. D. Li, L. L. Gu, Z. Lou, Z. Y. Fan, G. Z. Shen, *ACS Nano* **2017**, *11*, 4067.

[34] M. L. Lu, C. W. Lai, H. J. Pan, C. T. Chen, P. T. Chou, Y. F. Chen, *Nano Lett.* **2013**, *13*, 1920.

[35] Y. M. Li, Y. Song, Y. C. Jiang, M. X. Hu, Z. C. Pan, X. J. Xu, H. Y. Chen, Y. S. Li, L. F. Hu, X. S. Fang, *Adv. Funct. Mater.* **2017**, *27*, 1701066.

[36] R. Woods-Robinson, J. K. Cooper, X. J. Xu, L. T. Schelhas, V. L. Pool, A. Faghaninia, C. S. Lo, M. F. Toney, I. D. Sharp, J. W. Ager, *Adv. Electron. Mater.* **2016**, *2*, 1500396.

[37] S. K. Maurya, Y. Liu, X. J. Xu, R. Woods-Robinson, C. Das, J. W. Ager, K. R. Balasubramaniam, *J. Phys. D: Appl. Phys.* **2017**, *50*, 505107.

[38] X. J. Xu, J. Bullock, L. T. Schelhas, E. Z. Stutz, J. J. Fonseca, M. Hettick, V. L. Pool, K. F. Tai, M. F. Toney, X. S. Fang, A. Javey, L. H. Wong, J. W. Ager, *Nano Lett.* **2016**, *16*, 1925.

[39] X. J. Xu, S. Shukla, Y. Liu, B. B. Yue, J. Bullock, L. X. Su, Y. M. Li, A. Javey, X. S. Fang, J. W. Ager, *Phys. Status Solidi RRL* **2018**, *12*, 1700381.

[40] K. Hu, H. Y. Chen, M. M. Jiang, F. Teng, L. X. Zheng, X. S. Fang, *Adv. Funct. Mater.* **2016**, *26*, 6641.

[41] C. H. Liu, A. Piyadasa, M. Piech, S. Dardona, Z. Ren, P. X. Gao, *J. Mater. Chem. C* **2016**, *4*, 6176.

1800213 (7 of 7)